

A statistical analysis of the influence of vertical and ground speed errors on conflict probe

Jean-Marc Alliot* Nicolas Durand† Géraud Granger‡

CENA§

CENA

CENA

Keywords: air traffic control, conflict probe, statistical analysis.

Abstract

Conflict probes will be important components of air traffic control tools in the next years. They appear in almost every project (CINCAT, ERATO, HIPS, PHARE, and so on). To be useful, they have to fulfill two goals : reliability (they have to detect all conflicts) and efficiency (they must minimize the number of false alarms). Conflict probes rely on trajectory prediction, and their reliability and efficiency highly depend on the accuracy of trajectory prediction. In this paper, we present a quick mathematical insight of the influence of ground speed errors on trajectory prediction, results of arithmetic simulations on real traffic both on ground and vertical speed errors, and a statistical analysis of these results to model the influence of vertical and ground speed errors on conflict probe.

1 A mathematical overview

In this section, we present quickly some mathematical results regarding two aircraft conflict.

1.1 Two aircraft conflict at constant speed

Figure 1 show a classical two aircraft conflict. Aircraft on the lower segment fly at speed \vec{v}_1 , and aircraft on the upper segment fly at speed \vec{v}_2 . The angle of incidence is α .

We will use the auxiliary variables $r = v_2/v_1$, and D the separation standard. Let's suppose that we have an aircraft p_1 on the lower segment at a distance l_1 of the crossing point. We want to know which interval on the

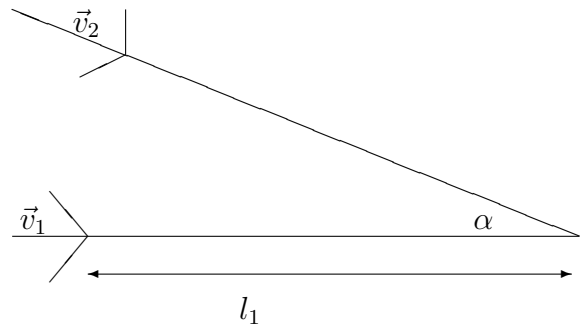


Figure 1: Two aircraft conflict

upper segment will contain conflicting aircraft with this one. Let's assume that an aircraft p_2 is at distance l_2 of the crossing point. Then we have (with a classical orthonormal referential):

$$\begin{aligned} x_1 &= v_1 t - l_1 \\ y_1 &= 0 \\ x_2 &= \cos(\alpha)(v_2 t - l_2) \\ y_2 &= \sin(\alpha)(l_2 - v_2 t) \end{aligned}$$

If the two aircraft are to be in conflict, there must exist t such that the following inequality is satisfied :

$$(x_1 - x_2)^2 + (y_1 - y_2)^2 \leq D^2$$

This is a second degree inequality in t . We notice that for $t \rightarrow +\infty$ or $t \rightarrow -\infty$, the inequality is not satisfied. So, it will only be satisfied if the equation:

$$(x_1 - x_2)^2 + (y_1 - y_2)^2 - D^2 = 0$$

has at least one root. If the discriminant of the above equation

$$\Delta = D^2(v_1^2 - 2v_1v_2 \cos(\alpha) + v_2^2) - \sin(\alpha)^2(l_2v_1 - l_1v_2)^2$$

is negative, then aircraft p_2 will never be in conflict with p_1 ; if the discriminant is positive, they will be in conflict during $[t_1, t_2]$ where t_1 and t_2 are the roots of the equation.

*e-mail: alliot@recherche.enac.fr

†e-mail: durand@recherche.enac.fr

‡e-mail: granger@recherche.enac.fr

§Centre d'Etudes de la Navigation Aérienne, 7 av Ed Belin, 31055 Toulouse, France

The discriminant is itself a polynomial of degree 2 in l_2 . Thus, the distances l_2 which satisfy $\Delta \geq 0$ belong to a single interval, and the extremal points of the interval are the roots of the equation $\Delta = 0$

$$r_1 = l_1 \frac{v_2}{v_1} + D \frac{\sqrt{1 + (\frac{v_2}{v_1})^2 - 2(\frac{v_2}{v_1}) \cos(\alpha)}}{\sin(\alpha)} \quad (1)$$

$$r_2 = l_1 \frac{v_2}{v_1} - D \frac{\sqrt{1 + (\frac{v_2}{v_1})^2 - 2(\frac{v_2}{v_1}) \cos(\alpha)}}{\sin(\alpha)} \quad (2)$$

However, we are only interested in the length of the segment, which is the difference between the two roots. We do not take into account the degenerate cases $\alpha = 0$ (takeover) and $\alpha = \pi$ (facing aircraft). It comes:

$$L = 2D \frac{\sqrt{1 + (v_2/v_1)^2 - 2(v_2/v_1) \cos(\alpha)}}{\sin(\alpha)}$$

We take $r = v_2/v_1$ as the ratio of speed and we express the length of the segment in number of separation standard:

$$\frac{L}{D} = f(r, \alpha) = 2 \frac{\sqrt{1 + r^2 - 2r \cos(\alpha)}}{\sin(\alpha)}$$

The function doesn't depend on l_1 (it could have been expected) and the minimum is reached for $r = \cos(\alpha)$, and we have $f(\cos(\alpha), \alpha) = 2$. This is independent of α and perfectly normal: it represents aircraft p_2 at a distance $-D < d < D$ of the crossing point when aircraft p_1 is exactly at the crossing point.

We represent on figure 2 a contour plot of the above function. The x axis is r (the ratio of v_2/v_1); we use values of r ranging from 0.5 to 1.5. The y axis is the angle of incidence α in degrees, from 20 degrees to 150 degrees. We do not represent values above 150 degrees or below 20 degrees, as they exhibit pathological behavior. These curves are not exactly new, as quite similar ones already appeared in documents describing the Gentle Strict (GS) algorithm of the AREA project[NFC+83, Nie89b, Nie89a]!

The darkest part of the contour plot represents segment lengths ranging from 2 to 2.5 separation standard. Each line represent one half separation standard more.

One should naively expect the function to be symmetrical with $f(r, \alpha) = f(1/r, \alpha)$, as the problem looks symmetrical: aircraft on the upper segment should "see" the same number of conflicts with aircraft on the lower segment than aircraft on the lower segment with aircraft on the upper segment. Actually, we have: $f(\frac{1}{r}, \alpha) = \frac{1}{r} f(r, \alpha)$. This can be intuitively understood on a simple example.

Let's suppose that aircraft on the upper and the lower segment are equally spaced by exactly one separation standard (maximal rate). Each aircraft on the lower segment

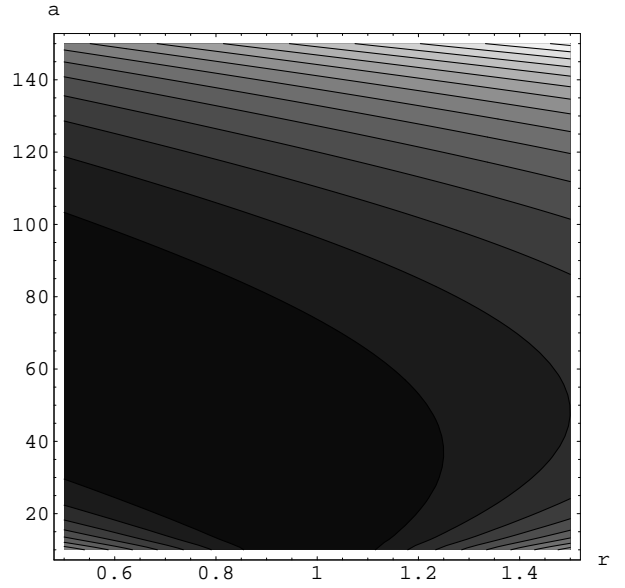


Figure 2: Two aircraft conflict

will detect roughly $f(r, \alpha)$ conflicts; in a given time period T , $n_1 = T \times (\frac{v_1}{D})$ aircraft will pass on the lower segment and the total number of conflicts detected by aircraft on the lower segment will be $n_1 f(r, \alpha)$. During the same time period, aircraft on the upper segment will detect $n_2 f(\frac{1}{r}, \alpha)$ conflicts. These two numbers have to be equal, so: $n_1 f(r, \alpha) = n_2 f(\frac{1}{r}, \alpha)$, or $f(r, \alpha) = \frac{n_2}{n_1} f(\frac{1}{r}, \alpha)$. By replacing n_1 and n_2 by their values:

$$f(r, \alpha) = \frac{T \times (\frac{v_2}{D})}{T \times (\frac{v_1}{D})} f(\frac{1}{r}, \alpha) = \frac{v_2}{v_1} f(\frac{1}{r}, \alpha) = r f(\frac{1}{r}, \alpha)$$

1.2 Two aircraft conflict with uncertainties

We suppose now that speeds are not exactly known, but that they belong to a given interval, with a percentage of error. We have then:

$$\begin{aligned} x_1 &= v_1(1 + e_1)t - l_1 \\ y_1 &= 0 \\ x_2 &= \cos(\alpha)(v_2(1 + e_2)t - l_2) \\ y_2 &= \sin(\alpha)(l_2 - v_2(1 + e_2)t) \end{aligned}$$

By taking the following variable: $r = \frac{v_2}{v_1}$, $l = \frac{l_1}{D}$ and $k = \frac{1+e_2}{1+e_1}$, we just have to substitute in equations 1 and 2 to get the new extremal points of the segment:

$$\frac{r_1}{D} = lkr + \frac{\sqrt{1 + r^2 k^2 - 2rk \cos(\alpha)}}{\sin(\alpha)}$$

$$\frac{r_2}{D} = lkr - \frac{\sqrt{1 + r^2 k^2 - 2rk \cos(\alpha)}}{\sin(\alpha)}$$

If we suppose that both e_1 and e_2 belongs to the same interval $[-e, e]$, we would like to plot the length of the segment as a function of e :

$$\frac{L}{D}(\alpha, l, r, e) = \max_{k \in [\frac{1-e}{1+e}, \frac{1+e}{1-e}]} \left[\frac{r_1}{D} \right] - \min_{k \in [\frac{1-e}{1+e}, \frac{1+e}{1-e}]} \left[\frac{r_2}{D} \right]$$

Let's consider the maximization of $r_1(k)$. It is a constrained maximization problem, so the extremum will be either on the hull of the convex (here at one of the points $\frac{1-e}{1+e}$ or $\frac{1+e}{1-e}$) or at an extremal point in the convex. This last point will be found by solving the equation:

$$\frac{\partial r_1}{\partial k} = lr + \frac{kr^2 - r \cos(\alpha)}{\sin \alpha \sqrt{1 + k^2 r^2 - 2kr \cos(\alpha)}} = 0$$

This equation has only one root in k :

$$k_r = \frac{-l\sqrt{1 - l^2 \sin^2 \alpha} \sin^2 \alpha + (1 - l^2 \sin^2 \alpha) \cos \alpha}{r(1 - l^2 \sin^2 \alpha)}$$

and this root only exists when $l < \frac{1}{\sin \alpha}$. The second order derivative is:

$$\frac{\partial^2 r_1}{\partial k^2} = \frac{r^2 \sin(\alpha)}{(1 + k^2 r^2 - 2kr \cos(\alpha))^{\frac{3}{2}}} > 0$$

We have also:

$$\begin{aligned} \frac{\partial r_1}{\partial k}(k=0) &= r\left(l - \frac{1}{\sin \alpha}\right) \\ \lim_{k \rightarrow \infty} \frac{\partial r_1}{\partial k}(k) &= r\left(l + \frac{1}{\sin \alpha}\right) \end{aligned}$$

Then we can conclude that the extremum of the function will never be reached inside the interval, but only at the upper or lower bound. Then:

$$\begin{aligned} l > \frac{1}{\sin \alpha} &: \max_{k \in [\frac{1-e}{1+e}, \frac{1+e}{1-e}]} \left[\frac{r_1}{D} \right] = \frac{r_1(\frac{1+e}{1-e})}{D} \\ l < \frac{1}{\sin \alpha} &: \max_{k \in [\frac{1-e}{1+e}, \frac{1+e}{1-e}]} \left[\frac{r_1}{D} \right] = \max \left\{ \frac{r_1(\frac{1+e}{1-e})}{D}, \frac{r_1(\frac{1-e}{1+e})}{D} \right\} \end{aligned}$$

An extremely similar discussion arises from the minimization of r_2 . The conclusion is:

$$\begin{aligned} l > \frac{1}{\sin \alpha} &: \min_{k \in [\frac{1-e}{1+e}, \frac{1+e}{1-e}]} \left[\frac{r_2}{D} \right] = \frac{r_2(\frac{1-e}{1+e})}{D} \\ l < \frac{1}{\sin \alpha} &: \min_{k \in [\frac{1-e}{1+e}, \frac{1+e}{1-e}]} \left[\frac{r_2}{D} \right] = \min \left\{ \frac{r_2(\frac{1+e}{1-e})}{D}, \frac{r_2(\frac{1-e}{1+e})}{D} \right\} \end{aligned}$$

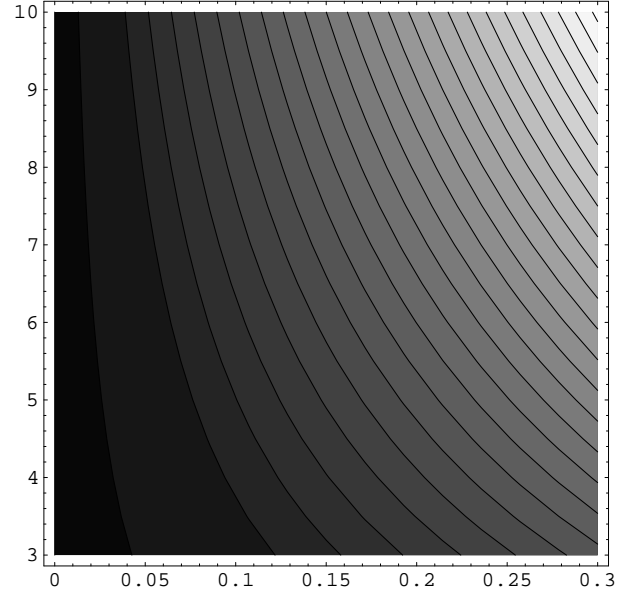


Figure 3: percentage of additional conflicts ($r=1, \alpha = \pi/4$)

We can now plot the length of the segment $\frac{L}{D}(\alpha, l, r, e)$. However, it is much more interesting here to represent the ratio of the number of conflicts detected (which is proportional to L) to the number of conflicts which would be detected if there was no uncertainty. So we do plot the function $\frac{L(\alpha, l, r, e)}{L(\alpha, l, r, 0)}$ on figure 3.

The x -axis is the uncertainty e with values from 0 to 30%; the y -axis is l , and is also the time to the crossing point in minutes if we make the approximation that an aircraft flies one separation standard in one minute; values range from 3 to 10 minutes to the crossing point. We set $r = 1$ and $\alpha = \pi/4$. The darkest part (on the left) is the zone where we have from 0 to 10% conflict more. Each line crossed towards the lightest zone adds 10% of conflict.

For example, if we detect conflicts 5 minutes before the crossing point, with an angle of convergence of 45 degrees, a speed ratio of 1 and an uncertainty of 15%, we will detect 50% more conflicts than if uncertainty was 0.

Notice that the time used is not the time before the start of the conflict but before the crossing point is reached. The difference is quite small for large values of α , but large for small values of α .

If we suppose that we detect conflicts far enough from the crossing point (a reasonable assumption), the maximum of r_1 is $r_1(\frac{1+e}{1-e})$ and the minimum of r_2 is $r_2(\frac{1-e}{1+e})$.

Then we have:

$$\frac{L}{D}(\alpha, l, r, e) = \frac{r_1(\frac{1+e}{1-e})}{D} - \frac{r_2(\frac{1-e}{1+e})}{D}$$

We can develop this equation:

$$\frac{L}{D} = \frac{4erl}{1-e^2} + \frac{1}{\sin(\alpha)} \left(\sqrt{1 + \frac{(1-e)^2 r^2}{(1+e)^2} - \frac{2(1-e)r \cos(\alpha)}{1+e}} + \sqrt{1 + \frac{(1+e)^2 r^2}{(1-e)^2} - \frac{2(1+e)r \cos(\alpha)}{1-e}} \right)$$

It is interesting to notice that the second term doesn't contain l and that for large values of l , this function is equivalent to $\frac{4erl}{1-e^2}$. For values of e not too large, we can write the order 1 Taylor series in e :

$$\frac{L}{D}(\alpha, r, l, e) = 4lre + 2 \frac{\sqrt{1+r^2-2r \cos(\alpha)}}{\sin(\alpha)}$$

and find back in the second term the length of the segment when $e = 0$ that was computed in the previous section. For that case, the increase in the number of conflicts is:

$$\begin{aligned} \frac{L(\alpha, r, l, e)}{L(\alpha, r, l, 0)} &= 1 + \frac{2r \sin(\alpha)}{\sqrt{1+r^2-2r \cos(\alpha)}} le \\ &= 1 + C(r, \alpha) le \end{aligned}$$

This last expression is simple and interesting. The 1 represents the "standard" number of conflicts, and the second term is the increase in percentage. Figure 4 is a contour plot of $C(r, \alpha)$ for $r \in [0.5, 1.5]$ and $\alpha \in [20, 150]$ degrees. The white zone corresponds to $1.9 < C(r, \alpha) < 2$, and each line crossed towards the darkest zone decreases $C(r, \alpha)$ by 0.1. The general shape of the curve is not surprising: for very small ($\simeq 0$) or very high ($\simeq 180$) values of α , conflicts are almost certain, so the percentage of "false alarms" remains small. Regarding the speed ratio, aircraft having quite similar speeds are intuitively more prone to give false alarms than aircraft with clearly different speeds.

On a simple numerical example ($r = 1$, $\alpha = 30$), we have:

$$\frac{L(\alpha, r, l, e)}{L(\alpha, r, l, 0)} \simeq 1 + 2le$$

where l can be considered as the time in minutes to the crossing point (with, again, the approximation that an aircraft fly one separation standard in one minute), and e is the uncertainty. for very small values of e ($e < 0.05$, i.e. 5%), the second term remains less than 1, even for l up to 10 minutes. However, for larger values of e , the function looks like $2le$, a direct proportionality to l and e .

The last two curves (figure 3 and 4) are extremely interesting. Acceptance of conflict probe systems depends highly on their efficiency, and this efficiency can be evaluated as the percentage of "false alarms". The theoretical

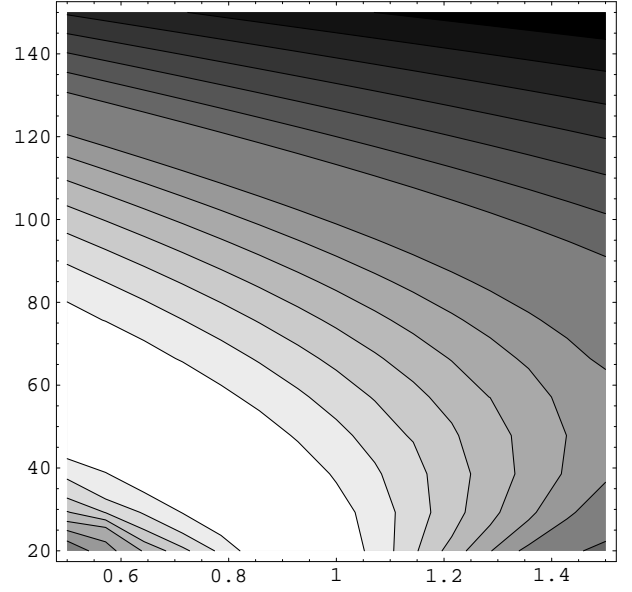


Figure 4: $C(r, \alpha)$

model shows that, to be able to detect conflicts soon and efficiently, we must be sure that the uncertainties on speed are as small as possible, and certainly less than 5%.

2 A statistical analysis

2.1 Introduction

The mathematical model makes lot of assumptions (constant speeds for example), many of them being quite unrealistic. Moreover, we haven't taken into account the vertical plane. We are now going to try to find a statistical model of the number of conflicts detected depending on the value of vertical and ground speed errors and of the value of the anticipation (the time window used for conflict detection).

To get data for our statistical analysis, simulations were used. The following subsections describe the experimental protocol.

2.2 The Air Traffic simulator

We used the OPAS [DAB97, DABM97] simulator (sometimes known as CATS) for simulations. It uses a tabulated model for aircraft performances: ground speed, vertical speed, and fuel burn are functions of altitude, aircraft type and flight segment (cruise, climb or descent.) The main dataset for aircraft flight performance is the base

of aircraft data (BADA) performance summary tables derived from the total energy model of EUROCONTROL. 69 different aircraft types are described. Synonym aircraft are used to model the rest of the fleet. The Airbus A320 (EA32) is used as default aircraft.

Aircraft follow classical routes (from way-point to way-point). The flight model is simple: an aircraft first climbs up to its RFL, then remains leveled till its top of descent, then descends to its destination.

Aircraft fly with a timestep that can be chosen at the start of the simulation. The timestep is always chosen in order to guarantee that two aircraft face to face flying at 500 kts could not cross without being closer than one standard separation at at least one timestep. For most of our simulation, we use a 15s timestep.

Flight plans are data of the COURAGE system, an archiving system of the operational French CAUTRA Air Traffic Control system. We have been using initial flight plans (without regulation), and we have used one of the module of the OPAS simulator to give slots to aircraft.

2.3 Conflict detection

Trajectory prediction is done *each three minutes* by a simulation of a given duration inside the global simulation. This duration is what we call the *anticipation*.

We assume during each of these detection simulations that there is an error about the aircraft future location because of ground and vertical speed prediction uncertainties.

Then, an aircraft is represented by a point at the initial time of the conflict detection window. But the point becomes a line segment in the uncertainty direction (the speed direction here, see figure 5). The first point of the line “flies” at the maximum possible speed, and the last point at the minimum possible speed. These maximal and minimal speeds depend of course on the uncertainty chosen: for 5% uncertainty on ground speed, the first point will fly at a speed of $1.05v$ and the last point at $0.95v$, if v is the nominal speed of the aircraft.

When changing direction on a beacon, the heading of the line segment “fastest point” changes as described on figure 5.

To check the standard separation at time t , we compute the distance between the two line segments modeling the aircraft positions and compare it to the standard separation at each timestep of the simulation.

In the vertical plane, we use a cylindrical modeling (figure 5). Each aircraft has a mean altitude, a maximal altitude and a minimal altitude. To check if two aircraft are in conflict, the minimal altitude of the higher aircraft is compared to the maximal altitude of the lower aircraft. The separation standard used is 6 nautical miles in the horizon-

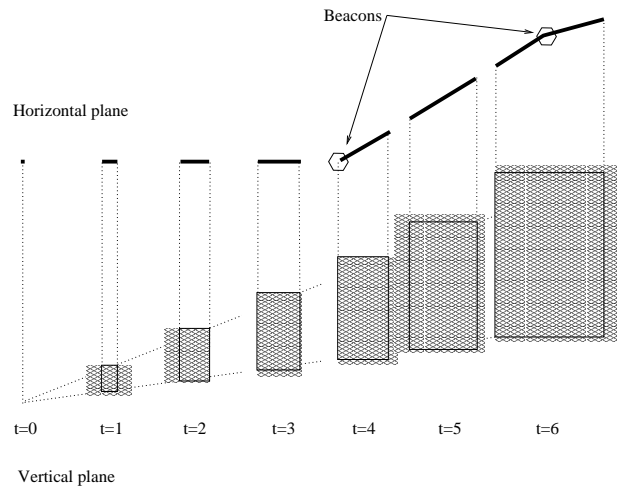


Figure 5: Modeling of speed uncertainties (standard routes).

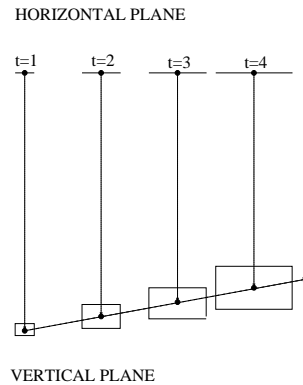


Figure 6: Modeling of speed uncertainties (direct routes).

tal plane and, 1000 ft under FL295 and 2000 ft above (no RVSM) in the vertical plane.

Conflicts detected can be merged: if a conflict is detected a time t_1 , and detected again three minutes later, the two conflicts are only considered as one. We maintain a hash table during the whole simulation to determine which conflicts are to be merged.

When using direct routes, the model is slightly modified (see figure 6) and much more simple. As aircraft never change direction, the aircraft is, at the beginning of the time window, a simple point, which becomes a line segment whose size grows with the uncertainty on speed. The modeling in the vertical plane is identical to the one used for standard routes.

t_w	e_g	e_v	N_d	N_s
0	0.00	0.00	1726	2758
4	0.02	0.01	2211	4001
4	0.02	0.40	3323	6264
4	0.16	0.01	4501	13653
4	0.16	0.40	6006	17847
12	0.02	0.01	2937	6474
12	0.16	0.40	14216	68200

Table 1: Results of simulations

2.4 Results

We ran 540 simulations with anticipation ranging from 4 minutes to 12 minutes, vertical speed error ranging from 1 to 40% and ground speed error ranging from 2 to 16%. In table 1, we give a very short sample of data found by simulations.

t_w is the duration of the time window in minutes, e_g is the horizontal uncertainty and e_v is the vertical uncertainty. N_d is the number of conflicts measured for these values for direct routes and N_s for standard routes.

It must be noticed (these results are not shown in the table) that when $t_w = 0$, $N = 1726$ for every value of e_g and e_v (when no predictions are made, there can't be more conflicts), and that $N = 1726$ also for all values of t_w when both e_g and e_v are equal to 0 (without uncertainties, conflicts can be detected from the beginning).

2.5 Statistical modeling (direct routes)

The problem when doing statistical analysis is to fit the data into the models that can be built and evaluated. In the first two subsections, we describe simple multiplicative models whose parameters can be easily found with linear regression (by using the logarithm), while in the third section we present a more complex model, requiring more elaborate methods to find the parameters.

2.5.1 A simple multiplicative model

In order to be able to use simple statistic methods, we tried the following modeling:

$$N = N_0 + a_0 t_w^{a_1} (1 + e_g)^{a_2} (1 + e_v)^{a_3}$$

t_w , e_g , e_v and N are the variables described in the subsection above, while N_0 is the number of conflicts when $t_w = e_g = e_v = 0$.

Using logarithms, we get:

$$\begin{aligned} \log(N - N_0) &= \log(a_0) + a_1 \log(t_w) + \\ & a_2 \log(1 + e_g) + a_3 \log(1 + e_v) \end{aligned}$$

	Estimate	SE	Tstat	PValue
$\log(a_0)$	5.068	0.0278	182	0
a_1	0.917	0.0122	75	0
a_2	10.78	0.1225	88	0
a_3	2.075	0.0444	47	0
$R^2 = 0.946689$				

Table 2: $N = N_0 + a_0 t_w^{a_1} (1 + e_g)^{a_2} (1 + e_v)^{a_3}$

We can then use a linear regression on all our data samples. These results are summarized in table 2. Results look good if we consider the statistical estimators presented [Sap90]: good R^2 , high T_s for all variables with a low probability value. However, this model works on the logarithm of all variables. An other standard, but more interesting (and intuitive), estimator of the validity of the model is:

$$S_e = \sqrt{\frac{\sum_{i=1}^{i=n_o} (N_i - \hat{N}_i)^2}{n_o}}$$

where n_o is the total number of observations, N_i is the number of conflicts observed, and \hat{N}_i is the number of conflicts predicted by the model.

S_e can be "interpreted" as a quadratic mean of the differences between observed values and predicted values.

For that model, we have $S_e = 487$, which is not a so small value if we consider that the actual number of conflicts range from 1726 to 14216.

Another indicator is:

$$s_e = \sqrt{\frac{\sum_{i=1}^{i=n_o} (1 - \frac{N_i}{\hat{N}_i})^2}{n_o}}$$

The S_e indicator has the disadvantage of giving more weights to large values, while this one estimates a global "percentage" of error. For this model, we have $s_e = 0.12$, a quite large value again.

Moreover, this model has a major problem. With both e_g and e_v equals to zero, we should get $N = N_0$, but this is not the case.

2.5.2 Another multiplicative model

Another model is:

$$N = N_0 + a_0 t_w^{a_1} e_g^{a_2} e_v^{a_3}$$

Using logarithms, we get:

$$\log(N - N_0) = \log(a_0) + a_1 \log(t_w) + a_2 \log(e_g) + a_3 \log(e_v)$$

Linear regression results are summarized in table 3. There again statistical results look good, but the computation of

	Estimate	SE	Tstat	PValue
$\log(a_0)$	8.49	0.0398	213	0
a_1	0.917	0.0144	64	0
a_2	0.694	0.00924	75	0
a_3	0.183	0.00503	37	0

$$R^2 = 0.959123$$

Table 3: $N = N_0 + a_0 t_w^{a_1} e_g^{a_2} e_v^{a_3}$

S_e and s_e gives $S_e = 453$ and $s_e = 0.12$, values extremely close to the one found for the other multiplicative model. This model corrects the problem above, but a new one arises: with this formula, having $e_g = 0$ or $e_v = 0$ will give $N = N_0$, which is, of course, incorrect.

2.5.3 A multiplicative and additive model

The two models above both exhibit congenital problems. We would like to have a model which gives $N = N_0$ only when $t_w = 0$ with any value of e_g or e_v , or when $e_g = 0$ and $e_v = 0$ with any value of t_w .

The simplest model having these two features is:

$$N = N_0 + a_0 t_w^{a_1} (e_g^{a_2} + a_3 e_v^{a_3})$$

But this model is both multiplicative and additive: we can not use standard regression methods to find the optimal values of the parameters.

The usual method is then to try to find the set of parameters minimizing the S_e or the s_e functions described above. We finally decided to optimize s_e .

We used both global optimization (interval arithmetic and branch and bound) and local optimization (simplex) to find the optimal set of parameters [Han92]. We finally get (when dividing by N_0):

$$\frac{N}{N_0} = 1 + t_w^{0.908} (3.66 e_g^{1.083} + 0.48 e_v^{0.973})$$

For that set of parameters and that model, we have $s_e = 0.048$, an excellent value, much lower than the values found for the other two models.

When $e_v = 0$, the increase of the number of conflict given by this model is almost identical to the formula found in the theoretical part of this paper. Exponents of t_w and e_g are extremely close to 1.

We notice that the exponent of e_v is also almost equal to 1, but this term has a lesser contribution, only 1/7 of the e_g contribution. We can try to explain this result: aircraft are stable during a large part of their flight, so the vertical uncertainty only has an influence during a smaller part of the flight than the horizontal uncertainty.

2.6 Statistical modeling (standard routes)

In this section, we consider the problems on standard routes. We only compute results for the best model, i.e. the additive and multiplicative one.

2.6.1 A model for standard routes

We now apply the following model:

$$N = N_0 + a_0 t_w^{a_1} (e_g^{a_2} + a_3 e_v^{a_3})$$

to the results found on standard routes.

We used exactly the same methods than above to find the parameters of the model. Then, we have:

$$\frac{N}{N_0} = 1 + t_w^{1.216} (8.05 e_g^{1.277} + 0.53 e_v^{1.180})$$

We have here $s_e = 0.058$, an excellent fit again.

We are still quite close to the theoretical model, but we must note some differences: the exponents are slightly larger than 1 (closer to 1.2), but the most striking fact is the value of the constant of the ground speed error. While it remains the same for vertical speed error (around 0.5), it is more than twice the direct route model value for ground speed error (8.05 instead of 3.66). This is easy to understand: as aircraft fly on routes, there are much more problems of takeover and face to face.

3 Conclusion

In this paper, we have presented a theoretical model and a statistical analysis of the influence of the vertical and ground speed errors on conflict probe.

The formulas which summarizes this study can be written approximatively:

$$\begin{aligned} \frac{N_d}{N_0} &= 1 + t_w (3.5 e_g + 0.5 e_v) \\ \frac{N_s}{N_0} &= 1 + t_w^{1.2} (8 e_g^{1.2} + 0.5 e_v^{1.2}) \end{aligned}$$

where $\frac{N}{N_0}$ represents the ratio of conflicts detected over conflicts really happening (N_d is the formula for direct routes, and N_s the formula for standard routes), t_w being the prediction anticipation, e_g being the ground speed error (in percentage) and e_v being the vertical speed error (in percentage also).

This model shows that, if we want to detect conflicts 10 minutes before they appear, and accept to detect twice the actual number of conflicts, we would need, for example to have $e_g < 0.014 = 1.4\%$ and $e_v < 0.1 = 10\%$

on direct routes; these values are currently out of reach of ground based trajectory prediction systems without using FMS informations.

The study also shows that improving significantly trajectory prediction will drastically reduce the number of conflicts detected, thus giving the controller a significant increase in his comfort, and probably a significant increase also in sector capacity.

These might be tracks that could be followed in the near future.

Biography

Jean-Marc Alliot graduated from the Ecole Polytechnique de Paris in 1986 and from the Ecole Nationale de l'Aviation Civile (ENAC) in 1988. He also holds a Ph.D. in Computer Science (1992). He is currently in charge of the global optimization laboratory of CENA and ENAC in Toulouse.

Nicolas Durand graduated from the Ecole Polytechnique de Paris in 1990 and from the Ecole Nationale de l'Aviation Civile (ENAC) in 1992. He has been a design engineer at the Centre d'Etudes de la Navigation Aérienne (CENA) since 1992 and holds a Ph.D. in computer Science (1996).

Géraud Granger graduated from the Ecole Nationale de l'Aviation Civile (ENAC) in 1998. He is completing a Ph.D. in Computer Science at the Ecole Polytechnique de Paris.

References

- [DAB97] Nicolas Durand, Jean-Marc Alliot, and Jean-François Bosc. Cats, a complete air traffic simulator. In *Proceedings of DASC97*, 1997.
- [DABM97] Nicolas Durand, Jean-Marc Alliot, Jean-François Bosc, and Lionel Maugis. An experimental study of atm capacity. In *Proceedings of Europe-USA conference on Air Traffic Management*, 1997.
- [Han92] Eldon Hansen. *Global optimizations using interval analysis*. Dekker, 1992. ISBN: 0-8247-8696-3.
- [NFC+83] W.P. Niedringhaus, I. Frolow, J.C. Corbin, A.H. Gisch, N.J. Taber, and F.H. Leiber. Automated En Route Air Traffic Control Algorithmic Specifications: Flight Plan Conflict Probe. Technical report, FAA, 1983. DOT/FAA/ES-83/6.

[Nie89a] W.P. Niedringhaus. Automated planning function for AERA3: Manoeuver Option Manager. Technical report, FAA, 1989. DOT/FAA/DS-89/21.

[Nie89b] W.P. Niedringhaus. A mathematical formulation for planning automated aircraft separation for AERA3. Technical report, FAA, 1989. DOT/FAA/DS-89/20.

[Sap90] Gilbert Saporta. *Probabilités, analyse des données et statistique*. Technip, 1990.